Finite-temperature theory of local environment effects in amorphous and liquid magnetic alloys

Y. Kakehashi
Department of Physics, Hokkaido Institute of Technology, Teine-Maeda, Teine-ku, Sapporo 006, Japan
(Received 27 November 1989)

A finite-temperature theory of magnetism that takes into account the fluctuations of local magnetic moments due to structural disorder is presented on the basis of the functional-integral method and the method of the distribution function. The theory describes qualitatively or semiquantitatively the finite-temperature magnetism of liquid and amorphous metals and alloys as well as the substitutional alloys in a wide range of electron-electron interaction strength from metal to insulator. The results of numerical calculations are presented for amorphous iron. The local environment effects on the density of states, local magnetic moment, susceptibility, and amplitude of local moment are examined. It is found that amorphous iron forms an itinerant-electron spin glass at low temperatures because of the nonlinear magnetic coupling between Fe local moments and the local environment effect on the amplitude of the Fe local moment due to the structural disorder. The calculated spin-glass temperature (100 K) is in good agreement with the value extrapolated from experimental data on Fe-rich amorphous alloys.

I. INTRODUCTION

Theoretical investigations of magnetic alloys with structural disorder are indispensable for understanding a variety of magnetic properties of amorphous and liquid alloys. In the past twenty years most of the effort has been concentrated on the description of the ground-state electronic structures and related magnetism.[1-9] We have now the best single-site approximation, which is called the effective-medium approximation (EMA).[2] In this theory a k-dependent effective medium describes the structural disorder on the electronic structure via the pair-distribution function. Realistic calculations[3] have also been performed by combining the EMA with the KKR (Korringa-Kohn-Rostker) method in energy-band theory.

When we want to describe the ground-state electronic structure going beyond the single-site approximation, we can adopt the recursion method[4] combined with the linear-muffin-tin-orbital method.[5] This approach[6,7] allows for a direct and first-principles calculation for any type of lattice structure. An alternative approach,[8,9] in which we directly diagonalize the one-electron Hamiltonian with a considerable number of atoms in a box with periodic boundary conditions has also been developed, and has become useful with the development of supercomputers.

The next step is to develop a finite-temperature theory of magnetism for amorphous and liquid alloys. This is especially important for transition metals and alloys in which the thermal spin fluctuations govern the local moment as well as itinerant-electron behavior at finite temperatures.[10]

We have recently proposed the first single-site theory at finite temperatures[11] on the basis of the functional integral method developed by Cyrot,[12] Hubbard,[13] and Hasegawa.[14] The theory interpolates between the weak and strong Coulomb interaction limits, and bridges the ground-state electronic structure and the magnetism at finite temperatures.

Although the single-site theory explains the change of the Curie constants at the melting point in transition metals and alloys, it completely neglects the fluctuations of the local magnetic moment (LM) due to structural disorder. Thus, it does not describe the spin glass (SG) as recently found in amorphous Fe-Zr and Fe-La alloys.[15-18]

In this paper we propose a finite-temperature theory of local environment effects (LEE) in liquid and amorphous alloys, which describes the fluctuations of the LM's due to structural disorder, therefore, the SG in amorphous alloys. Several years ago we developed the theory of LEE for substitutional alloys.[19,20] It explained qualitatively or semiquantitatively the SG state, the Slater-Pauling curves, and the Curie temperature Slater-Pauling curves in $3d$ transition-metal alloys.[19-26] The present theory is an extension of the previous theory, but treats a new type of disorder, i.e., the structural disorder as well as the configurational disorder.

In the following section we present our theory. We first review the two-field functional-integral method[27] to describe the thermal spin fluctuations. We then derive an expression of the LM in an effective medium according to our physical picture. The treatment of the structural disorder on the electronic structure will be given in Sec. III C. In Sec. III D the LM distribution produced by the structural and configurational disorders will be treated by means of the method of distribution function initiated by Matsubara[28] and Katsura *et al.*[29] Simplified self-consistent equations which allow for the numerical calculations will be presented in Sec. III E.

This work was motivated by the recent discovery of the

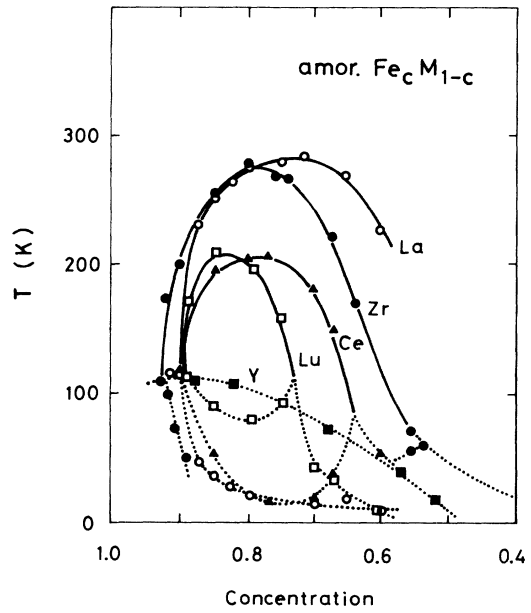

FIG. 1. Experimental magnetic phase diagram (Ref. 30) showing the Curie temperatures (solid curves) and the spin-glass temperatures (dotted curves) in amorphous Fe_cM_{1-c} alloys (M =La, Zr, Ce, Lu, and Y).

SG state in Fe-rich amorphous alloys[15–18,30] as shown in Fig. 1. The alloys show the SG with a high transition temperature. Though the SG states are found also in the fcc $(Fe_cNi_{1-c})_{92}C_8$ and $(Fe_cNi_{1-c})_{80}Cr_{20}$ alloys,[31,32] an important characteristic in Fe-rich amorphous alloys is that they have the same transition temperature at more than 90 at. % Fe irrespective of the second elements. This suggests that the Fe-rich amorphous alloys provide us with the first example of the SG produced by the structural disorder instead of the configurational disorder. Moreover, it suggests a new possibility of the SG phase in amorphous pure iron. In Sec. III we investigate the finite-temperature magnetism of amorphous iron by using the present theory of LEE. We will examine the role of the LEE on the magnetism of amorphous iron, and theoretically show that the SG is realized at low temperatures in amorphous iron. A part of this section has been published as a letter.[33] In the last section we will summarize our results and discuss the magnetism of amorphous iron in comparison with the recent ground-state calculations.[34]

II. THEORY OF LEE

A. Functional-integral method

The finite-temperature magnetism in the intermediate regime between weak and strong interaction limits is well known to be described qualitatively or semiquantitatively by the functional-integral method.[10,12–14] We briefly review in this subsection the functional-integral technique to the degenerate-band Hubbard model,[27] and present some results which will be used in the following sections.

We start from the degenerate-band Hubbard model[35,36] with Hund's rule coupling, and adopt the two-field functional-integral method to take into account the thermal spin fluctuations. In this method the interacting Hamiltonian is transformed into a one-electron system with time-dependent fictitious fields acting on each site.[37,38] Within the static approximation in which the time dependence of the fields is neglected, the free energy F is written as follows:

$$F=-\beta^{-1}\ln\int\left[\prod_{i=1}^{N}\left[\frac{\beta\tilde{J}_i}{4\pi}\right]^{1/2}d\xi_i\right]e^{-\beta E(\xi)}\ . \tag{2.1}$$

Here β is the inverse temperature, $\tilde{J}_i$ is an effective-exchange energy parameter defined by

$$\tilde{J}_i=\frac{1}{2D}U_i+\left[1+\frac{1}{2D}\right]J_i\ , \tag{2.2}$$

U_i (J_i) being a Coulomb (exchange) integral on site i. D denotes the degeneracy of the bands (e.g., $D=5$ for $3d$ transition metals).

The energy functional $E(\xi)$ in Eq. (2.1) consists of the free energy for the one-electron Hamiltonian $H(\xi)$ with the exchange fields $\{\xi_i\}$ and the Gaussian terms

$$E(\xi)=-\beta^{-1}\ln\mathrm{tr}(e^{-\beta H(\xi)})-\sum_i\tfrac{1}{4}[\tilde{U}_i\zeta_i(\xi)^2-\tilde{J}_i\xi_i^2]\ . \tag{2.3}$$

Here $\tilde{U}_i$ is an effective Coulomb integral defined by

$$\tilde{U}_i=\left[1-\frac{1}{2D}\right]U_i+\frac{1}{2D}J_i\ . \tag{2.4}$$

$\zeta_i(\xi)$ in the Gaussian term denotes an average electron number on site i with respect to $H(\xi)$.

The one-electron Hamiltonian $H(\xi)$ in Eq. (2.3) is expressed as

$$H(\xi)=\sum_{i\nu\sigma}(\varepsilon_i^0-\mu+\tfrac{1}{2}\tilde{U}_i\zeta_i-\tfrac{1}{2}\tilde{J}_i\xi_i\sigma-h_i\sigma)n_{i\nu\sigma}+\sum_{ij\nu\sigma}t_{ij}'a_{i\nu\sigma}^{\dagger}a_{j\nu\sigma}\ . \tag{2.5}$$

Here ε_i^0 and h_i are the atomic level and external magnetic field on site i, respectively. μ is the chemical potential. t_{ij}' denotes the transfer integral between sites i and j. $a_{i\nu\sigma}^{\dagger}$ ($a_{i\nu\sigma}$) is the creation (annihilation) operator for electrons with spin σ on site i and orbital ν. Furthermore, $n_{i\nu\sigma}=a_{i\nu\sigma}^{\dagger}a_{i\nu\sigma}$.

The thermal average of LM and the amplitude of LM on site i are obtained by differentiating the free energy F with respect to h_i and J_i (Ref. 27)

$$\langle m_i\rangle=\langle\xi_i\rangle\ , \tag{2.6}$$

$$\langle m_i^2\rangle=3\langle\zeta_i\rangle-\frac{3}{2D}\langle\xi_i^2\rangle+\left[1+\frac{1}{2D}\right]\left[\langle\xi_i^2\rangle-\frac{2}{\beta\tilde{J}_i}\right]\ . \tag{2.7}$$

Here, $\langle\cdots\rangle$ on the right-hand side (rhs) means a classical average with respect to $E(\xi)$:

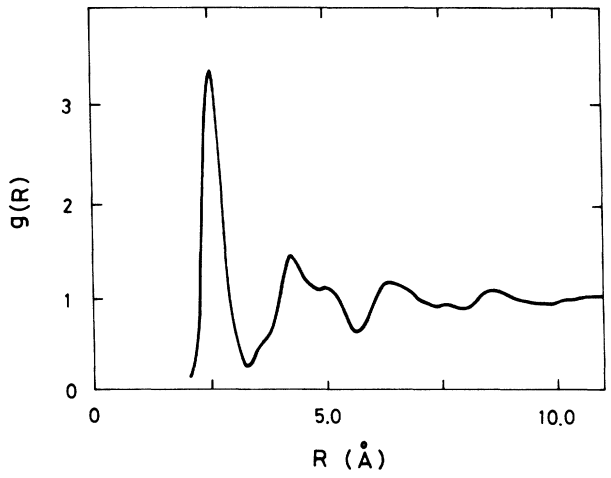

FIG. 2. Pair-distribution function of computer-generated amorphous iron (Ref. 40).

$$\langle \cdots \rangle = \frac{\int \left[\prod_i d\xi_i\right] (\cdots) e^{-\beta E(\xi)}}{\int \left[\prod_i d\xi_i\right] e^{-\beta E(\xi)}} . \tag{2.8}$$

In order to simplify the actual calculations we consider a limit $\tilde{U}_i \to \infty$, introducing charge potentials $\{w_i(\xi)\}$ (Ref. 13). These potentials are determined by the charge neutrality condition on each site. Furthermore, we adopt the transfer integrals described by a geometrical average: $t'_{ij} = r_i^* t_{ij} r_j$, where t_{ij} is the transfer integral for a pure metal, and r_i is an off-diagonal factor[39] which depends on a type of atom on site i. Then Eq. (2.3) is written as follows (see the Appendix in Ref. 23):

$$E(\xi) = \int d\omega f(\omega) \frac{D}{\pi} \mathrm{Im\,tr}[\ln(L^{-1} - t)] + \sum_i [-n_i w_i(\xi) + \tfrac{1}{4}\tilde{J}_i \xi_i^2] . \tag{2.9}$$

Here $f(\omega)$ is the Fermi distribution function. t denotes the matrix t_{ij}. n_i is the electron number on site i. The locator L is defined by

$$(L^{-1})_{i\nu j\nu'\sigma} = L_{i\sigma}^{-1} \delta_{ij} \delta_{\nu\nu'} = \frac{\omega + i\delta - \varepsilon_i^0 - w_i(\xi) + \frac{1}{2}\tilde{J}_i \xi_i \sigma + \mu}{|r_i|^2} \delta_{ij} \delta_{\nu\nu'} . \tag{2.10}$$

Here δ in $\omega + i\delta$ means an infinitesimal positive number.

B. Local moments in an effective medium

In order to proceed with the formulation one needs a physical picture for the structure of amorphous and liquid alloys. We show in Fig. 2 the pair-distribution function for amorphous iron obtained from a computer simulation with use of realistic interatomic potentials.[40] The most important feature is that the first peak is very sharp and is well separated from the second and third peaks which are much broader than the first one. Recent experimental data of pair-distribution functions for amorphous $Fe_{90}La_{10}$ alloys[41] show a similar structure. This implies that there exists a well-defined nearest-neighbor (NN) shell even in amorphous and liquid alloys. Therefore, we take into account the LEE due to the nearest-neighbor atoms directly, and describe the structural disorder due to further distant atoms by using an effective medium as shown in Fig. 3.

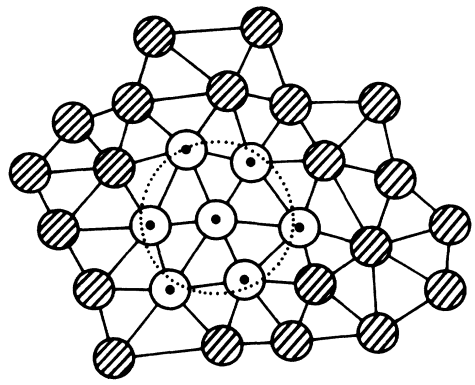

FIG. 3. Physical picture for amorphous and liquid structure. The central atom has a well-defined nearest-neighbor (NN) shell (dotted circle). Further distant atoms (hatched circles) are regarded as an effective medium.

Let us derive the expression of a central LM consistent with Fig. 3. The present system contains three kinds of disorder: the spin disorder due to thermal spin fluctuations, configurational disorder, and structural disorder. The first and second ones appear as a diagonal disorder in the locators (2.10), while the third one appears in both locators L and transfer integrals t.

We first introduce an inverse effective locator $\mathcal{L}_\sigma^{-1}$ into the first term in Eq. (2.9) to describe the diagonal disorder as an average medium and expand the deviation with respect to the sites. The zeroth order is described by the effective medium only. The first-order correction consists of the sum of single-site energy functionals $E_i(\xi_i)$:

$$E_i(\xi_i) = \int d\omega f(\omega) \frac{D}{\pi} \mathrm{Im} \sum_\sigma \ln(L_{i\sigma}^{-1} - \mathcal{L}_\sigma^{-1} + F_{ii\sigma}^{-1}) - n_i w_i(\xi) + \tfrac{1}{4}\tilde{J}_i \xi_i^2 , \tag{2.11}$$

$$F_{ij\sigma} = [(\mathcal{L}^{-1} - t)^{-1}]_{ij\sigma} . \tag{2.12}$$

In the next term the pair-interaction terms $\sum_{(i,j)} \Phi_{ij}(\xi_i, \xi_j)$ appear. $\Phi_{ij}(\xi_i, \xi_j)$ denotes the pair energy functional between sites i and j:

$$\Phi_{ij}(\xi_i, \xi_j) = \int d\omega f(\omega) \frac{D}{\pi} \mathrm{Im} \sum_\sigma \ln[1 - F_{ij\sigma} F_{ji\sigma} \tilde{t}_{i\sigma}(\xi_i) \tilde{t}_{j\sigma}(\xi_j)] . \tag{2.13}$$

Here $\tilde{t}_{i\sigma}(\xi_i)$ is the single-site t matrix defined by

$$\tilde{t}_{i\sigma}(\xi_i)=\frac{L_{i\sigma}^{-1}-\mathcal{L}_{\sigma}^{-1}}{1+(L_{i\sigma}^{-1}-\mathcal{L}_{\sigma}^{-1})F_{i\sigma}} . \tag{2.14}$$

All higher-order terms are neglected in the present theory by assuming small deviation from the effective medium. The approximation has been justified for substitutional transition-metal alloys[22-26] by comparing the local densities of states (DOS) at low temperatures with those in the cluster CPA (coherent-potential approximation).[42-44]

The energy functional $E(\xi)$ in Eq. (2.9) is then expressed as follows:

$$E(\xi)=\sum_i E_i(\xi_i)+\sum_{(i,j)}\Phi_{ij}(\xi_i,\xi_j) . \tag{2.15}$$

Here we have dropped the zeroth term since it does not make any contribution to the thermal averages (2.6) and (2.7).

In the next step we treat the thermal average in Eq. (2.6). Since the direct integration of the type (2.8) is impossible, we replace the surrounding exchange-field variables $\{\xi_j\}$ by the Ising spins $\{s_j=\pm 1\}$ making use of the following decoupling approximation which is correct up to the second moment:

$$\langle \xi_j^{2n+k}\rangle_0=x_j^{2n}\langle \xi_j^k\rangle_0 \quad (k=0,1) , \tag{2.16}$$

where

$$\langle \xi_j^k\rangle_0=\int d\xi_j(\xi_j^k)\exp[-\beta E_j(\xi_j)]\Big/\int d\xi_j\exp[-\beta E_j(\xi_j)] , \tag{2.17}$$

and

$$x_j=\langle \xi_j^2\rangle_0^{1/2} . \tag{2.18}$$

Then we have[45]

$$\langle m_0\rangle=\frac{\sum_{\{s\}}\int d\xi_0\xi_0 e^{-\beta\Psi'(\xi_0,s_1x_1,s_2x_2,\dots)}}{\sum_{\{s\}}\int d\xi_0 e^{-\beta\Psi'(\xi_0,s_1x_1,s_2x_2,\dots)}} , \tag{2.19}$$

$$\Psi'(\xi_0,s_1x_1,s_2x_2,\dots)=E_0(\xi_0)+\sum_{i\neq 0}\Phi_{0i}^{(a)}(\xi_0)-\sum_{i\neq 0}\left[\Phi_{0i}^{(e)}(\xi_0)+\beta^{-1}\tanh^{-1}\frac{\langle \xi_i\rangle_0}{x_i}\sum_{j\neq 0,i}\mathcal{H}_{ij}\right]s_i-\sum_{(i,j)}{}'\mathcal{J}_{ij}s_is_j . \tag{2.20}$$

Here $\sum_{\{s\}}=\sum_{s_1}\sum_{s_2}\dots$, and $\sum'_{(i,j)}$ implies a summation with respect to all pairs which are not related to site 0. Pair interactions $\Phi_{0i}^{(a)}(\xi_0)$, $\Phi_{0i}^{(e)}(\xi_0)$, $\mathcal{H}_{ij}$, and $\mathcal{J}_{ij}$ are defined, respectively, as follows:

$$\begin{bmatrix}\Phi_{0i}^{(a)}(\xi_0)\\ \Phi_{0i}^{(e)}(\xi_0)\end{bmatrix}=\tfrac{1}{2}\sum_{\nu=\pm}\begin{bmatrix}1\\ -\nu\end{bmatrix}\Phi_{0i}(\xi_0,\nu x_i) , \tag{2.21}$$

$$\begin{bmatrix}\mathcal{H}_{ij}\\ \mathcal{J}_{ij}\end{bmatrix}=-\tfrac{1}{4}\sum_{\lambda=\pm}\sum_{\nu=\pm}\lambda\begin{bmatrix}1\\ \nu\end{bmatrix}\Phi_{ij}(\lambda x_i,\nu x_j) . \tag{2.22}$$

The coupling $\mathcal{J}_{ij}$ means an exchange-coupling energy between the atoms on sites i and j as seen from the last term on the rhs in Eq. (2.20).

In the following we make a molecular-field approximation for the thermal average; the variables s_i in Eq. (2.20) are replaced by their thermal averages $\langle s_i\rangle=\langle m_i\rangle/x_i$. Equations (2.19) and (2.20) reduce to

$$\langle m_0\rangle=\frac{\int d\xi\,\xi e^{-\beta\Psi(\xi)}}{\int d\xi e^{-\beta\Psi(\xi)}} , \tag{2.23}$$

$$\Psi(\xi)=E_0(\xi)+\sum_{i=1}^{z}\Phi_{0i}^{(a)}(\xi)-\sum_{i=1}^{z}\Phi_{0i}^{(e)}(\xi)\frac{\langle m_i\rangle}{x_i} . \tag{2.24}$$

Here z is the number of atoms on the NN shell. We took into account the pair interactions in the NN shell and neglected the direct interactions with the atoms outside the shell because of the damping effect in the disordered systems.[46] Furthermore, we replace, in the calculation of pair interactions (2.21), the inverse locators $L_{j\sigma}^{-1}$ on the NN shell by the configurational and structural average under a given type of atom α:

$$L_{\alpha\sigma}^{-1}(\omega+i\delta,\xi)=\frac{\omega+i\delta-\bar{\varepsilon}_\alpha+\mu-\bar{w}_\alpha(\xi)+\frac{1}{2}\tilde{J}_\alpha\xi\sigma}{|r_\alpha|^2} . \tag{2.25}$$

Here $\bar{\varepsilon}_\alpha$ and $\bar{w}_\alpha(\xi)$ denote the average atomic level and potential for atom α on site j.

The effective medium $\mathcal{L}_\sigma^{-1}$ is determined so that the averaged single-site t matrix vanishes:

$$[[\langle \tilde{t}_{0\sigma}(\xi)\rangle]_s]_c=0 . \tag{2.26}$$

Here $\langle\cdots\rangle$ means the thermal average with respect to $\Psi(\xi)$. $[\,]_c$ ($[\,]_s$) denotes the configurational (structural) average. Equation (2.26) is called the CPA equation.[47]

C. Treatment of structural disorder

The central LM (2.23) contains the structural disorder due to the atoms outside the cluster via the coherent Green functions $F_{00\sigma}$, $F_{0j\sigma}$, $F_{jj\sigma}$ in Eq. (2.24).

We first replace the diagonal Green functions $F_{jj\sigma}$ on the NN shell by their structural and configurational aver-

ages under the condition that the type of atom α on site j is fixed:

$$F_{\alpha\sigma}=[[F_{jj\sigma}]_s]_c=\int \frac{[[\rho_\alpha(\varepsilon)]_s]_c d\varepsilon}{\mathcal{L}_\sigma^{-1}-\varepsilon} . \tag{2.27}$$

Here the average DOS $[[\rho_\alpha(\varepsilon)]_s]_c$ for $\{t_{ij}\}$ might depend on the type of atom α on site j because of the difference in the size of atom.

For the central Green functions $F_{00\sigma}$ and $F_{j0\sigma}(=F_{0j\sigma})$, we adopt the Bethe approximation. By using the locator expansion we have the relations (see Fig. 4)

$$F_{00}=\mathcal{L}+\mathcal{L}\sum_{j\neq 0} t_{0j}F_{j0} , \tag{2.28}$$

$$F_{j0}=\mathcal{L}t_{j0}F_{00}+\mathcal{L}S_jF_{j0}+\mathcal{L}\sum_{i\neq j,0} T_{ji}F_{i0} . \tag{2.29}$$

Here we have omitted the spin suffix σ for brevity and neglected the transfer integrals to the atoms outside the NN shell. The self-energy S_j (T_{ji}) means the sum of all the paths which start from site j and end at site j (i) without returning to the cluster on the way. Note that all the information outside the cluster is contained in S_j and T_{ji}.

We neglect the last term on the rhs of Eq. (2.29), and replace S_j by $\mathcal{S}_{\gamma_j}$, an effective medium for the structural disorder. Here γ_j denotes the type of atom on site j. We then obtain

$$F_{00\sigma}=\left[\mathcal{L}_\sigma^{-1}-\sum_{j=1}^{z}\frac{t_{i0}^2}{\mathcal{L}_\sigma^{-1}-\mathcal{S}_{\gamma_j\sigma}}\right]^{-1} , \tag{2.30}$$

$$F_{j0\sigma}=\frac{t_{j0}}{\mathcal{L}_\sigma^{-1}-\mathcal{S}_{\gamma_j\sigma}}F_{00\sigma} . \tag{2.31}$$

An improvement of this part might be possible by using a method proposed by Miwa.[48]

The effective medium $\mathcal{S}_{\alpha\sigma}$ ($\alpha=A$ or B) is determined from the condition that the structural and configurational averages of the central coherent Green function $F_{00\sigma}$ should be identical with the neighboring ones ($[[F_{jj\sigma}]_s]_c$):

$$[[F_{\alpha\alpha\sigma}]_s]_c=\int \frac{[[\rho_\alpha(\varepsilon)]_s]_c d\varepsilon}{\mathcal{L}_\sigma^{-1}-\varepsilon} \tag{2.32}$$

Here $F_{\alpha\alpha\sigma}$ denotes $F_{00\sigma}$ when the site 0 is occupied by the atom of type α. The DOS $[[\rho_\alpha(\varepsilon)]_s]_c$ on the rhs of Eq. (2.32) can be accurately calculated by using the recursion method.[6,7]

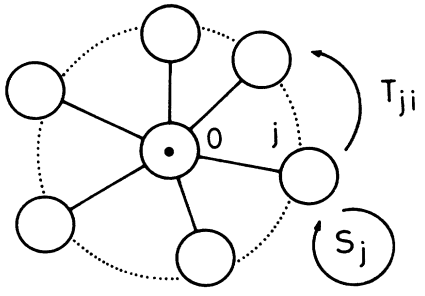

FIG. 4. Schematic representation of the irreducible paths S_j and T_{ji}.

D. Method of distribution function

After introducing the effective medium ($\mathcal{L}_\sigma^{-1}$ and $\mathcal{S}_{\alpha\sigma}$), Eq. (2.23) realizes the central LM with a NN shell as shown in Fig. 3. The central LM is then determined by the surrounding LM's $\{\langle m_j\rangle\}$, the atomic configuration on the NN shell $\{\gamma_j\}$, and the transfer integrals $\{y_j=t_{0j}^2\}$ between the central atom and the atoms on the NN shell. (See Fig. 5).

We introduce here the probability $p_c^{\alpha\gamma}$ of finding γ atom at the neighboring site when the central site is occupied by atom α, and the probability $p_s^{\alpha\gamma}(y)dy$ that the square of the transfer integral between atoms α and γ takes a value in the regime $(y, y+dy)$. The former is given by Cowley's atomic short-range order parameter[49] τ as

$$p_c^{\alpha\gamma}=c_\gamma+(\delta_{\alpha\gamma}-c_\gamma)\tau ,$$

c_γ being the concentration of atom α. The latter is obtained from the experimental pair-distribution function and the dependence of t_{j0} on the interatomic distance R.

The distributions of $\{\gamma_j\}$ and $\{y_j\}$ cause the LM distribution $g_\alpha(\langle m_0\rangle)$ at the central site via Eq. (2.23). Since the same distribution holds true for the surrounding LM's $\{\langle m_j\rangle\}$, we obtain an integral equation to determine the distribution $g_\alpha(M)$ via Eq. (2.23) as follows (see also Fig. 5).

Let us assume that the central site is occupied by atom α and there are no correlations between the atoms on the NN shell. Under this assumption the probability that a set of surrounding LM's $\{\langle m_j\rangle\}$ with the atomic configuration $\{\gamma_j\}$ is between $\{m_j\}$ and $\{m_j+dm_j\}$ and a set of $\{t_{j0}^2\}$ is between $\{y_j\}$ and $\{y_j+dy_j\}$, is given by

$$\prod_{j=1}^{z}[p_c^{\alpha\gamma_j}p_s^{\alpha\gamma_j}(y_j)dy_j g_{\gamma_j}(m_j)dm_j] .$$

Then the central LM takes a value $\langle m_\alpha\rangle(\{\langle m_j\rangle\},\{\gamma_j\},\{y_j\})$ via Eq. (2.23). Therefore, the probability that the central LM takes a value between M and $M+\Delta M$ is given by

$$g_\alpha(M)\Delta M=\sum_{\{\gamma_j\}}\int_{M\le\langle m_\alpha\rangle\le M+\Delta M}\prod_{j=1}^{z}[p_c^{\alpha\gamma_j}p_s^{\alpha\gamma_j}(y_j)dy_j g_{\gamma_j}(m_j)dm_j] . \tag{2.33}$$

Inserting $\int dM'\delta(M'-\langle m_\alpha\rangle)=1$ into the rhs of Eq. (2.33) and classifying the atomic configuration according to the number of atoms α on the NN shell, we obtain

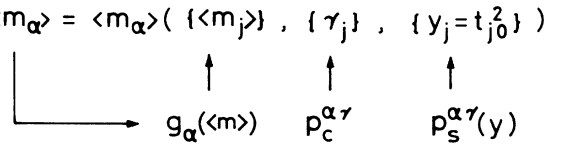

FIG. 5. Schematic representation for the method of distribution function in amorphous and liquid alloys. See the text for $g_\alpha(\langle m\rangle)$, $p_c^{\alpha\gamma}$, and $p_s^{\alpha\gamma}(y)$.

$$g_\alpha(M)=\sum_{n=0}^{z}\Gamma(n,z,p_c^{\alpha\alpha})\int\delta(M-\langle m_\alpha\rangle)\prod_{i=1}^{n}[p_s^{\alpha\alpha}(y_i)dy_i g_\alpha(m_i)dm_i]\prod_{j=n+1}^{z}[p_s^{\alpha\bar{\alpha}}(y_j)dy_j g_{\bar{\alpha}}(m_j)dm_j]\ . \tag{2.34}$$

Here $\Gamma(n,z,p)$ is the binomial distribution function defined by

$$[z!/n!(z-n)!]p^n(1-p)^{z-n}\ .$$

In the same way Eqs. (2.26) and (2.32) are written, respectively, as follows:

$$\sum_\alpha c_\alpha\sum_{n=0}^{z}\Gamma(n,z,p_c^{\alpha\alpha})\int\langle\tilde{t}_{\alpha\sigma}\rangle\prod_{i=1}^{n}[p_s^{\alpha\alpha}(y_i)dy_i g_\alpha(m_i)dm_i]\prod_{j=n+1}^{z}[p_s^{\alpha\bar{\alpha}}(y_j)dy_j g_{\bar{\alpha}}(m_j)dm_j]=0\ , \tag{2.35}$$

$$\sum_{n=0}^{z}\Gamma(n,z,p_c^{\alpha\alpha})\int F_{\alpha\alpha\sigma}\left[\prod_{i=1}^{n}p_s^{\alpha\alpha}(y_i)dy_i\right]\left[\prod_{j=n+1}^{z}p_s^{\alpha\bar{\alpha}}(y_j)dy_j\right]=\int\frac{[[\rho_\alpha(\varepsilon)]_s]_c d\varepsilon}{\mathcal{L}_\sigma^{-1}-\varepsilon}\ . \tag{2.36}$$

Here $\langle\tilde{t}_{\alpha\sigma}\rangle$ is the thermal average of the t matrix for the atom of type α at the central site, and $F_{\alpha\alpha\sigma}$ is defined by Eq. (2.30) in which the central site is occupied by atom α and there are n atoms of type α on the NN shell.

Equations (2.34)–(2.36) determine self-consistently the LM distribution $g_\alpha(M)$, the effective medium $\mathcal{L}_\sigma^{-1}$ for the diagonal disorder, and the effective medium $\mathcal{S}_{\alpha\sigma}$ for the structural disorder. The averaged LM for atom α and the SG order parameter are given as follows:

$$\begin{bmatrix}[[\langle m_\alpha\rangle]_s]_c\\ [[\langle m_\alpha\rangle^2]_s]_c\end{bmatrix}=\int dM\begin{bmatrix}M\\ M^2\end{bmatrix}g_\alpha(M)\ . \tag{2.37}$$

E. Simplified self consistent equations

Self-consistent equations (2.34)–(2.36) include $2z$-fold integrations on the rhs. Thus, we have to make some approximations which allow for the numerical calculations.

We adopt the following decoupling approximation on the rhs of Eqs. (2.34)–(2.36), which is correct up to the second moment:

$$\int M^{2n+k}g_\alpha(M)dM\approx[[\langle m_\alpha\rangle^2]_s]_c^n[[\langle m_\alpha\rangle^k]_s]_c\ , \tag{2.38}$$

$$\int(y-[y_{\alpha\gamma}]_s)^{2n+k}p_s^{\alpha\gamma}(y)dy\approx[(\delta y)^2_{\alpha\gamma}]_s^n 0^k\ . \tag{2.39}$$

Here $k=0$ or 1. $[y_{\alpha\gamma}]_s$ is an average transfer integral between atoms α and γ, $[(\delta y)^2_{\alpha\gamma}]_s$ is the fluctuation around $[y_{\alpha\gamma}]_s$ which is defined by

$$[(\delta y)^2_{\alpha\gamma}]_s=\int(y-[y_{\alpha\gamma}]_s)^2p_s^{\alpha\gamma}(y)dy\ . \tag{2.40}$$

This is calculated from the fluctuation of the interatomic distance R as follows:

$$\frac{[(\delta y)^2_{\alpha\gamma}]_s^{1/2}}{[y_{\alpha\gamma}]_s}=2\kappa\frac{[(\delta R)^2_{\alpha\gamma}]_s^{1/2}}{[R_{\alpha\gamma}]_s}\ . \tag{2.41}$$

Here we assumed $t_{\alpha\gamma}(R)\propto R^{-\kappa}$. $[R_{\alpha\gamma}]_s$ and $[(\delta R)^2_{\alpha\gamma}]_s^{1/2}$ denote the average interatomic distance between atoms α and γ and its fluctuation. They are estimated from the pair-distribution function.

Adopting Eqs. (2.38) and (2.39), on the rhs of Eq. (2.34) we obtain

$$g_\alpha(M)=\sum_{n=0}^{z}\sum_{i=0}^{n}\sum_{j=0}^{z-n}\sum_{k_1=0}^{i}\sum_{k_2=0}^{n-i}\sum_{l_1=0}^{j}\sum_{l_2=0}^{z-n-j}\Gamma(n,z,p_c^{\alpha\alpha})\Gamma(i,n,\tfrac{1}{2})\Gamma(j,z-n,\tfrac{1}{2})\Gamma(k_1,i,q_{\alpha+})\Gamma(k_2,n-i,q_{\alpha+})$$
$$\times\Gamma(l_1,j,q_{\bar{\alpha}+})\Gamma(l_2,z-n-j,q_{\bar{\alpha}+})\delta(M-\langle m_\alpha\rangle(n,i,j,k_1,k_2,l_1,l_2))\ . \tag{2.42}$$

Here

$$q_{\alpha+}=\frac{1}{2}\left[1+\frac{u_\alpha}{v_\alpha}\right]\ , \tag{2.43}$$

$$\langle m_\alpha\rangle(n,i,j,k_1,k_2,l_1,l_2)=\frac{\int d\xi\xi e^{-\beta\Psi_\alpha(\xi,nijk_1k_2l_1l_2)}}{\int d\xi e^{-\beta\Psi_\alpha(\xi,nijk_1k_2l_1l_2)}}\ , \tag{2.44}$$

$$\Psi_\alpha(\xi,nijk_1k_2l_1l_2)=E_\alpha(\xi,nij)+i\Phi^{(a)}_{\alpha\alpha-}(\xi,nij)+(n-i)\Phi^{(a)}_{\alpha\alpha+}(\xi,nij)+j\Phi^{(a)}_{\alpha\bar{\alpha}+}(\xi,nij)$$
$$+(z-n-j)\Phi^{(a)}_{\alpha\bar{\alpha}-}(\xi,nij)-(2k_1-i)\Phi^{(e)}_{\alpha\alpha+}(\xi,nij)v_\alpha-(2k_2-n+i)\Phi^{(e)}_{\alpha\alpha-}(\xi,nij)v_\alpha$$
$$-(2l_1-j)\Phi^{(e)}_{\alpha\bar{\alpha}+}(\xi,nij)v_{\bar{\alpha}}-(2l_2-z+n+j)\Phi^{(e)}_{\alpha\bar{\alpha}-}(\xi,nij)v_{\bar{\alpha}}\ , \tag{2.45}$$

and

$$u_\alpha x_\alpha=[[\langle m_\alpha\rangle]_s]_c,\quad v_\alpha x_\alpha=[[\langle m_\alpha\rangle^2]_s]_c^{1/2}\ . \tag{2.46}$$

In the present approximation the structural disorder is described via the NN transfer integrals by the contraction $(-[(\delta R)^2_{\alpha\gamma}]_s^{1/2})$ of the NN interatomic distance R from the average value $[R_{\alpha\gamma}]_s$ and the stretch $([(\delta R)^2_{\alpha\gamma}]_s^{1/2})$ of the distance R. Then we can specify the local structure and the atomic configuration in the cluster with a central atom of type α by means of the number of atoms (n) of type α on the NN shell, the number of contracted pairs (i) between the central atom of type α and the atoms of type α on the NN shell, and the number of contracted pairs (j) between the central atom α and the atoms $\bar{\alpha}$ on the NN shell. We call this state the (nij) configuration in the following. Note that there are $n-i$ stretched α-α pairs and $z-n-j$ stretched α-$\bar{\alpha}$ pairs between the central atom and the NN shell in this configuration.

The single-site energy functional at the central site $[E_\alpha(\xi,nij)$ in Eq. (2.45)] is then defined by Eq. (2.11) with the (nij) configuration. The pair energy $\Phi^{(a)}_{\alpha\gamma+}(\xi,nij)$ $[\Phi^{(a)}_{\alpha\gamma-}(\xi,nij)]$ denotes the atomic energy in Eq. (2.21) for a contracted (stretched) pair with (nij) configuration. The exchange pair energies $\Phi^{(e)}_{\alpha\gamma\pm}(\xi,nij)$ are defined in the same way.

Substituting Eq. (2.42) into the rhs of Eq. (2.37), we obtain the self-consistent equations for $[[\langle m_\alpha\rangle]_s]_c$ and $[[\langle m_\alpha\rangle^2]_s]_c$:

$$\begin{bmatrix}[[\langle m_\alpha\rangle]_s]_c\\ [[\langle m_\alpha\rangle^2]_s]_c\end{bmatrix}=\sum_{nijkl}\Gamma(nijk_1k_2l_1l_2)\begin{bmatrix}\langle m_\alpha\rangle(n,i,j,k_1,k_2,l_1,l_2)\\ \langle m_\alpha\rangle(n,i,j,k_1,k_2,l_1,l_2)^2\end{bmatrix}\ . \tag{2.47}$$

Here $\sum_{nijkl}$ means the sum

$$\sum_{n=0}^{z}\sum_{i=0}^{n}\sum_{j=0}^{z-n}\sum_{k_1=0}^{i}\sum_{k_2=0}^{n-i}\sum_{l_1=0}^{j}\sum_{l_2=0}^{z-n-j}\ ,$$

and $\Gamma(nijk_1k_2l_1l_2)$ is defined by

$$\Gamma(nijk_1k_2l_1l_2)=\Gamma(n,z,p_c^{\alpha\alpha})\Gamma(i,n,\tfrac{1}{2})\Gamma(j,z-n,\tfrac{1}{2})\Gamma(k_1,i,q_{\alpha+})\Gamma(k_2,n-i,q_{\alpha+})\Gamma(l_1,j,q_{\bar{\alpha}+})\Gamma(l_2,z-n-j,q_{\bar{\alpha}+})\ . \tag{2.48}$$

Within the same approximation the CPA equation (2.35) reduces to the following equation:

$$\sum_\alpha c_\alpha\sum_{nijkl}\Gamma(nijk_1k_2l_1l_2)\frac{\int d\xi e^{-\beta\Psi_\alpha(\xi,nijk_1k_2l_1l_2)}\tilde{t}_{\alpha\sigma}(\xi,nij)}{\int d\xi e^{-\beta\Psi_\alpha(\xi,nijk_1k_2l_1l_2)}}=0\ . \tag{2.49}$$

Here $\tilde{t}_{\alpha\sigma}(\xi,nij)$ is the single-site t matrix (2.14) in the (nij) configuration.

Since the effective medium is not expected to be sensitive to the details of the structure, we replace $F_{00\sigma}$ and $L_{0\sigma}^{-1}$ in $\tilde{t}_{\alpha\sigma}(\xi,nij)$ by the averaged ones [i.e., Eqs. (2.25) and (2.27)]. Furthermore, we adopt the following decoupling approximation in Eq. (2.49):

$$[[\langle\xi_\alpha^{2n+k}\rangle]_s]_c\approx[[\langle\xi_\alpha^2\rangle]_s]_c^n[[\langle\xi_\alpha^k\rangle]_s]_c\quad(k=0,1)\ . \tag{2.50}$$

Here the averages are defined by

$$[[\langle\xi_\alpha^m\rangle]_s]_c=\sum_{nijkl}\Gamma(nijk_1k_2l_1l_2)\langle\xi_\alpha^m\rangle(nijk_1k_2l_1l_2)\ , \tag{2.51}$$

$$\langle\xi_\alpha^m\rangle(nijk_1k_2l_1l_2)=\frac{\int d\xi\xi^m e^{-\beta\Psi_\alpha(\xi,nijk_1k_2l_1l_2)}}{\int d\xi e^{-\beta\Psi_\alpha(\xi,nijk_1k_2l_1l_2)}}\ . \tag{2.52}$$

Note that

$$\langle\xi_\alpha\rangle(nijk_1k_2l_1l_2)=\langle m_\alpha\rangle(n,i,j,k_1,k_2,l_1,l_2)\ .$$

Finally, CPA equation (2.49) is simplified as follows:

$$\sum_\alpha c_\alpha\sum_\nu\frac{1}{2}\left[1+\nu\frac{[[\langle\xi_\alpha\rangle]_s]_c}{[[\langle\xi_\alpha^2\rangle]_s]_c^{1/2}}\right]\frac{L_{\alpha\sigma}^{-1}(\omega+i\delta,\nu[[\langle\xi_\alpha^2\rangle]_s]_c^{1/2})-\mathcal{L}_\sigma^{-1}}{1+\{L_{\alpha\sigma}^{-1}(\omega+i\delta,\nu[[\langle\xi_\alpha^2\rangle]_s]_c^{1/2})-\mathcal{L}_\sigma^{-1}\}F_{\alpha\sigma}}=0\ . \tag{2.53}$$

Next we simplify Eq. (2.36) for the effective medium $\mathcal{S}_{\alpha\sigma}$. Let us note that the structural disorder in the coherent Green function $F_{\alpha\alpha\sigma}$ appears only via the variables $\theta_{\alpha\alpha}=\sum_{i=1}^n y_i$ and $\theta_{\alpha\bar{\alpha}}=\sum_{i=n+1}^z y_i$ as follows:

$$F_{\alpha\alpha\sigma}=(\mathcal{L}_\sigma^{-1}-\theta_{\alpha\alpha}K_{\alpha\sigma}-\theta_{\alpha\bar{\alpha}}K_{\bar{\alpha}\sigma})^{-1} . \tag{2.54}$$

Here

$$K_{\alpha\sigma}=(\mathcal{L}_\sigma^{-1}-\mathcal{S}_{\alpha\sigma})^{-1} . \tag{2.55}$$

We again adopt the decoupling approximation for $\delta\theta_{\alpha\gamma}=\theta_{\alpha\gamma}-[\theta_{\alpha\gamma}]_s$:

$$[(\delta\theta_{\alpha\gamma})^{2n+k}]_s\approx[(\delta\theta_{\alpha\gamma})^2]_s^n[(\delta\theta_{\alpha\gamma})^k]_s \quad (k=0,1) . \tag{2.56}$$

Then we have

$$[F_{\alpha\alpha\sigma}]_s=\tfrac{1}{4}\sum_{\nu=\pm}\sum_{\nu'=\pm}\{\mathcal{L}_\sigma^{-1}-n[y_{\alpha\alpha}]_sK_{\alpha\sigma}-(z-n)[y_{\alpha\bar{\alpha}}]_sK_{\bar{\alpha}\sigma}-\nu\sqrt{n}\,[(\delta y)_{\alpha\alpha}^2]_s^{1/2}K_{\alpha\sigma}-\nu'\sqrt{z-n}\,[(\delta y)_{\alpha\bar{\alpha}}^2]_s^{1/2}K_{\bar{\alpha}\sigma}\}^{-1} . \tag{2.57}$$

Here we adopted the relations $[\theta_{\alpha\alpha}]_s=n[y_{\alpha\alpha}]_s$, $[\theta_{\alpha\bar{\alpha}}]_s=(z-n)[y_{\alpha\bar{\alpha}}]_s$, $[(\delta\theta_{\alpha\alpha})^2]_s=n[(\delta y)_{\alpha\alpha}^2]_s$, and $[(\delta\theta_{\alpha\bar{\alpha}})^2]_s=(z-n)[(\delta y)_{\alpha\bar{\alpha}}^2]_s$.

Taking the configurational average in Eq. (2.57) we obtain an equation for $K_{\alpha\sigma}$ which is simpler than Eq. (2.36):

$$\sum_{n=0}^{z}\Gamma(n,z,p_c^{\alpha\alpha})[F_{\alpha\alpha\sigma}]_s=F_{\alpha\sigma} . \tag{2.58}$$

The self-consistent equations (2.47), (2.53), and (2.58) determine the order parameters ($[[\langle m_\alpha\rangle]_s]_c$ and $[[\langle m_\alpha\rangle^2]_s]_c$) and the effective medium [$\mathcal{L}_\sigma^{-1}$ and $K_{\alpha\sigma}$ (or $\mathcal{S}_{\alpha\sigma}$)]. Once we determine the medium from these equations, we can calculate other physical quantities. For example, the amplitude of LM [see Eq. (2.7)] is given by

$$[[\langle \mathbf{m}_\alpha^2\rangle]_s]_c=\sum_{nijkl}\Gamma(nijk_1k_2l_1l_2)\langle \mathbf{m}_\alpha^2\rangle(nijk_1k_2l_1l_2) , \tag{2.59}$$

$$\langle \mathbf{m}_\alpha^2\rangle(nijk_1k_2l_1l_2)=3n_\alpha-\frac{3}{2D}n_\alpha^2+\left[1+\frac{1}{2D}\right]\left[\langle\xi_\alpha^2\rangle(nijk_1k_2l_1l_2)-\frac{2}{\beta\tilde{J}_\alpha}\right] . \tag{2.60}$$

In the substitutional alloys the present theory reduces to the previous theory of LEE for substitutional alloys.[20,23] In particular, the theory gives, in the local-moment limit, the well-known spin-glass temperature T_g of the molecular-field approximation[19,29]

$$T_g^2=\tfrac{1}{2}z\{c_A\mathcal{J}_{AA}^2+c_B\mathcal{J}_{BB}^2+[(c_A\mathcal{J}_{AA}^2-c_B\mathcal{J}_{BB}^2)^2+4c_Ac_B\mathcal{J}_{AB}^4]^{1/2}\} . \tag{2.61}$$

In the case of amorphous and liquid metals the self-consistent equation (2.47) reduces to

$$\begin{bmatrix}[\langle m\rangle]_s\\ [\langle m\rangle^2]_s\end{bmatrix}=\sum_{n=0}^{z}\Gamma(n,z,\tfrac{1}{2})\begin{bmatrix}[\langle m\rangle_n]_s\\ [\langle m\rangle_n^2]_s\end{bmatrix} , \tag{2.62}$$

$$\begin{bmatrix}[\langle m\rangle_n]_s\\ [\langle m\rangle_n^2]_s\end{bmatrix}=\sum_{k=0}^{n}\sum_{l=0}^{z-n}\Gamma(k,n,q)\Gamma(l,z-n,q)\begin{bmatrix}\langle\xi\rangle(nkl)\\ \langle\xi\rangle(nkl)^2\end{bmatrix} , \tag{2.63}$$

$$\langle\xi\rangle(nkl)=\frac{\int d\xi\,\xi e^{-\beta\Psi(\xi,nkl)}}{\int d\xi\,e^{-\beta\Psi(\xi,nkl)}} , \tag{2.64}$$

$$\Psi(\xi,nkl)=E(\xi,n)+n\Phi_+^{(a)}(\xi,n)+(z-n)\Phi_-^{(a)}(\xi,n)-[(2k-n)\Phi_+^{(e)}(\xi,n)+(2l-z+n)\Phi_-^{(e)}(\xi,n)]\frac{[\langle m\rangle^2]_s^{1/2}}{x} , \tag{2.65}$$

$$q=\frac{1}{2}\left[1+\frac{[\langle m\rangle]_s}{[\langle m\rangle^2]_s^{1/2}}\right] . \tag{2.66}$$

Here and in the following, the type of atom and other indicators are omitted.

The CPA equation (2.53) for the effective medium $\mathcal{L}_\sigma^{-1}$ reduces to

$$\sum_\nu\frac{1}{2}\left[1+\nu\frac{[\langle\xi\rangle]_s}{[\langle\xi^2\rangle]_s^{1/2}}\right]\{L_\sigma^{-1}(\omega+i\delta,\nu[\langle\xi^2\rangle]_s^{1/2})-\mathcal{L}_\sigma^{-1}+F_\sigma^{-1}\}^{-1}=F_\sigma . \tag{2.67}$$

Equation (2.58) to determine the medium for the structural disorder reduces to

$$\sum_{\nu} \tfrac{1}{2}\{\mathcal{L}_\sigma^{-1} - z[y]_s K_\sigma - \nu\sqrt{z}\,[(\delta y)^2]_s^{1/2} K_\sigma\}^{-1} = F_\sigma \ . \tag{2.68}$$

This equation can be solved analytically:

$$z[y]_s K_\sigma = \frac{2F_\sigma\mathcal{L}_\sigma^{-1} - 1 \pm \left[1 + 4\dfrac{[(\delta y)^2]_s}{z[y]_s^2} F_\sigma\mathcal{L}_\sigma^{-1}(F_\sigma\mathcal{L}_\sigma^{-1} - 1)\right]^{1/2}}{2\left[1 - \dfrac{[(\delta y)^2]_s}{z[y]_s^2}\right]F_\sigma} \ . \tag{2.69}$$

The sign on the rhs should be chosen to be $\mathrm{Im}K_\sigma < 0$. Equations (2.62), (2.67), and (2.69) determine the magnetic state for amorphous and liquid metals. The equations contain the spin-glass solution due to the structural disorder ($[\langle m\rangle]_s = 0$ and $[\langle m\rangle^2]_s \neq 0$). The spin-glass temperature is obtained analytically in the local-moment limit as follows:

$$T_g^2 = \tfrac{1}{2} z(\mathcal{J}_+^2 + \mathcal{J}_-^2) \ , \tag{2.70}$$

where $\mathcal{J}_+$ ($\mathcal{J}_-$) is the exchange coupling (2.22) for contracted (stretched) pair. It reduces to the well-known formula[50,51]

$$T_g = \sqrt{z}\,|\mathcal{J}| \ , \tag{2.71}$$

for $\mathcal{J} = \mathcal{J}_+ = -\mathcal{J}_-$ (i.e., $\pm\mathcal{J}$ model).

Equations (2.61) and (2.71) indicate that the present theory automatically includes both types of SG: the site and bond models in the insulator limit.

III. NUMERICAL RESULTS FOR AMORPHOUS IRON

We present the result of the calculation for amorphous iron as a numerical example in this section. Our aim is to clarify the possibility of the SG in amorphous iron.

We adopted the d-electron number $n = 7.0$ per iron atom, the exchange-energy parameter $\tilde{J} = 0.059\,045$ Ry, and the best result of the averaged d DOS $[\rho(\varepsilon)]_s$ by Fujiwara.[52] The latter is shown in Fig. 6 together with the bcc and fcc DOS.[53] The exchange-energy parameter $\tilde{J}$ is chosen so as to reproduce the observed ground-state magnetization $2.216\mu_B$ for the bcc Fe. (See Fig. 7.) The averaged transfer integral $[y]_s$ was calculated from the relation

$$z[t^2]_s = \int (\varepsilon - \varepsilon_0)^2 [\rho(\varepsilon)]_s d\varepsilon \ .$$

The transfer integrals are assumed to be in proportion to $(1/R)^{3.8}$ (Ref. 54). The fluctuation of the interatomic distance was fixed to be $[(\delta R)^2]_s^{1/2}/[R]_s = 0.06$. This value is consistent with the value 0.067 which was estimated from the width of the first peak in the theoretical[40] and experimental[51] pair-distribution functions.

We solved the self-consistent equations in the following way. First we assume $[\langle m\rangle]_s$, $[\langle m\rangle^2]_s$, $[\langle\xi^2\rangle]_s$, and $w(\pm[\langle\xi^2\rangle]_s)$. We can then obtain the effective medium $\mathcal{L}_\sigma^{-1}$ solving the CPA equation (2.67). We calculate the effective medium K_σ for the structural disorder according to Eq. (2.69), and calculate $F_{00\sigma}$ and $F_{01\sigma}$ [Eqs. (2.30) and (2.31)] for various configurations of local structure. Next we obtain the charge potentials $\bar{w}(\xi)$ and $w(\xi,n)$ from the charge neutrality conditions, respectively,

$$n = \int d\omega f(\omega)\frac{D}{\pi}\,\mathrm{Im}[L_\sigma^{-1}(\omega + i\delta,\xi) - \mathcal{L}_\sigma^{-1} + F_\sigma^{-1}]^{-1} \ , \tag{3.1}$$

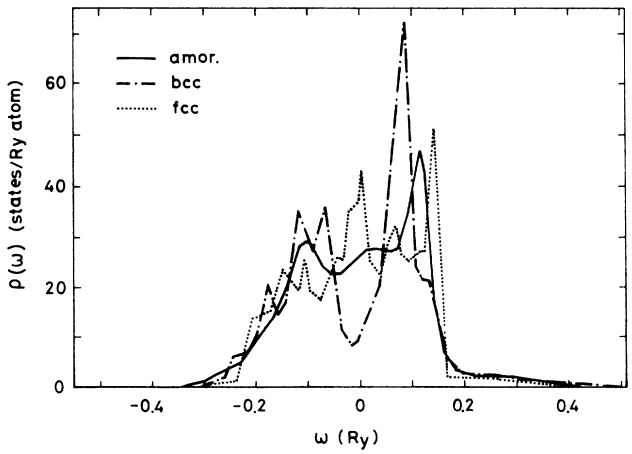

FIG. 6. The densities of states (DOS) for iron used in the present calculation. ——: amorphous iron (Ref. 52). —·—·—·: bcc iron (Ref. 52). · · · ·: fcc iron (Ref. 53).

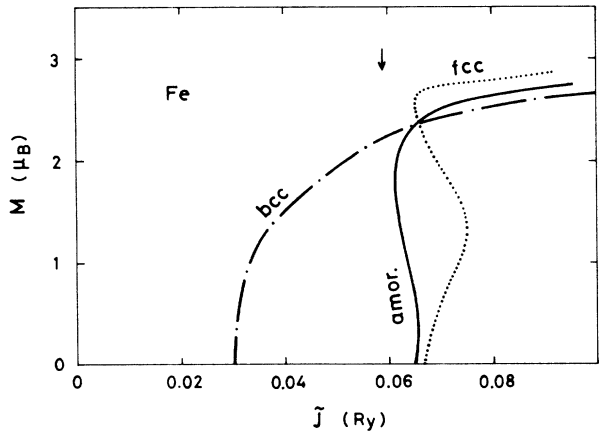

FIG. 7. Uniform ground-state magnetization (M) vs exchange-energy parameter ($\tilde{J}$) curves in the Stoner model. The DOS presented in Fig. 6 are used in the calculation. The arrow indicates the exchange-energy parameter ($\tilde{J} = 0.059\,045$ Ry) which leads to the ground-state magnetization $2.216\mu_B$ in the bcc Fe.

$$n=\int d\omega f(\omega)\frac{D}{\pi}\,\mathrm{Im}[L_\sigma^{-1}(\omega+i\delta,\xi)-\mathcal{L}_\sigma^{-1}+F_{00\sigma}^{-1}]^{-1}\ . \tag{3.2}$$

Next we calculate $x=\langle\xi^2\rangle_0^{1/2}$, $E(\xi,n)$, $\Phi_\pm^{(a)}(\xi,n)$, and $\Phi_\pm^{(e)}(\xi,n)$ by using $\mathcal{L}_\sigma^{-1}$, $w(\xi,n)$, $F_{00\sigma}$, $F_{01\sigma}$, and F_σ. Then we can solve Eq. (2.62) by means of the iteration method, and we have a new set of $[\langle m\rangle]_s$, $[\langle m\rangle^2]_s$, $[\langle\xi^2\rangle]_s$, and $w(\pm[\langle\xi^2\rangle]_s^{1/2})$. This procedure should be repeated until the self-consistency is achieved.

Figure 8 shows the calculated local DOS for the noninteracting electron system in various environments. The DOS with 12 contracted atoms ($n=12$) on the NN shell shows the double-peak structure with broad bandwidth, while the DOS with 0 contracted atom ($n=0$) shows the single peak with narrow band because the central atom is isolated from the surrounding atoms. The existence of the local DOS with single- and double-peak structures in various environments is consistent with the nonmagnetic results based on the recursion method by Fujiwara.[6]

When the electron-electron interaction $\tilde{J}$ is taken into account, the line shapes of the DOS are somewhat changed as shown in Fig. 9. The peaks around $\omega=0.05$ Ry in the DOS with $n=6$ and 12 are broadened because of thermal spin fluctuations. The DOS for isolated atoms ($n=0$) split into two peaks because of the LM formation due to electron-electron interaction in the narrow band. Thus, the local DOS is expected to show a double-peak structure irrespective of the environment.

Various local magnetic states change the averaged probability distribution $p(\xi)$ defined by $[\langle m\rangle]_s=\int d\xi p(\xi)\xi$. In Fig. 10 the probability distribution with LEE is compared with that in the single-site approximation.[11] The latter shows a simple two-peak structure corresponding to the double minima in the single-site energy functional. The former has a three-peak structure: a central peak due to the local structures with $n>10$ and the peaks at $\xi=\pm1.7\mu_B$ due to the local structures with $n<6$.

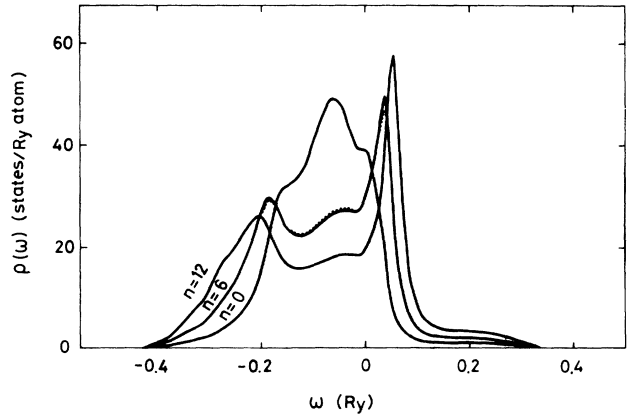

FIG. 8. Local DOS for noninteracting electrons in amorphous iron in various environments specified by the number of contracted atoms (n) on the NN shell. Dotted curves denote the averaged DOS (Ref. 52).

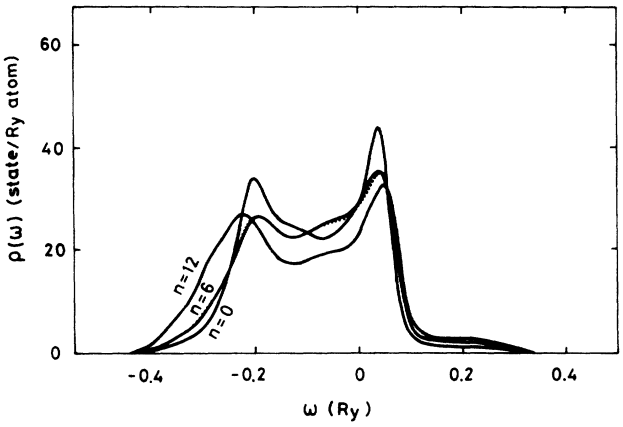

FIG. 9. Local DOS at $T=35$ K in various environments.

The uniform ferromagnetism is not expected in amorphous iron as seen from Fig. 7. We numerically checked that the ferromagnetism is not stable in amorphous iron even if we take into account the fluctuations of the LM's due to the structural disorder. Figure 11 presents the result for inverse susceptibility versus temperature curves. The inverse susceptibility follows the Curie-Weiss law at high temperatures, but becomes slightly convex upwards at less than about 700 K. The present result clearly shows the cusp at $T_g=92$ K for

$$[(\delta R)^2]_s^{1/2}/[R]_s=0.06$$

and $T_g=129$ K for

$$[(\delta R)^2]_s^{1/2}/[R]_s=0.07\ ,$$

below which the order parameter $[\langle m\rangle^2]_s^{1/2}$ develops with decreasing temperatures. The calculated SG temperature is in good agreement with the value (≈100 K) expected from the experimental data of Fe-rich amorphous alloys.[17,18,30] Although the theory is based on a molecular-field approximation, the present result for T_g

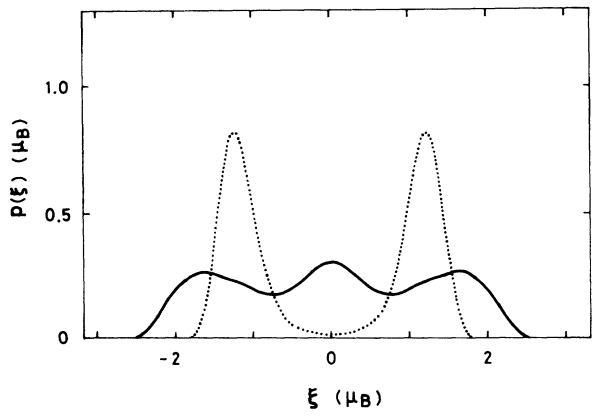

FIG. 10. Probability distribution $p(\xi)$ for the present theory (solid curve) and the single-site theory (dotted curve).

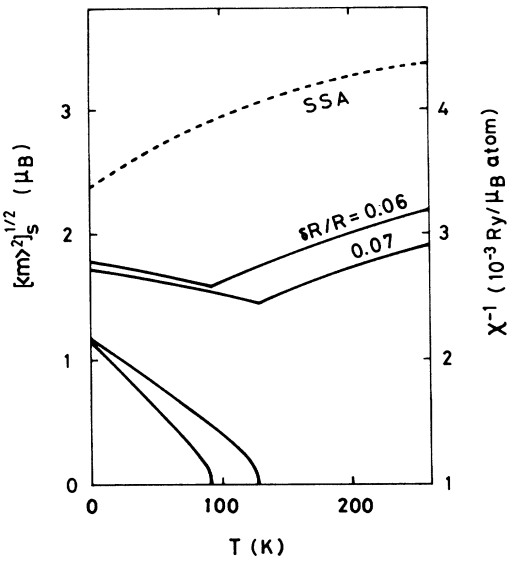

FIG. 11. The spin-glass order parameter ($[\langle m\rangle^2]_s^{1/2}$) and inverse susceptibilities as a function of temperature for $[(\delta R)^2]_s^{1/2}/[R]_s=0.06$ and 0.07. The dashed curve denotes the inverse susceptibility in the single-site approximation.

is expected to be reasonable because the frustration effect as seen in the spins on the fcc lattice is not important for the amorphous systems. Moreover, the existence of the SG in amorphous iron is not sensitive to the magnitude of $[(\delta R)^2]_s^{1/2}/[R]_s$ as shown in Fig. 12.

The inverse susceptibility in the single-site theory is overestimated by a factor of 1.5 as compared with the present result. (See Fig. 11.) This is because the single-site theory neglects the LM's with large amplitudes which remarkably enhance the susceptibility. It should also be pointed out that these is no cusp in the single-site theory because of no fluctuation ($[\langle m\rangle^2]_s=0$).

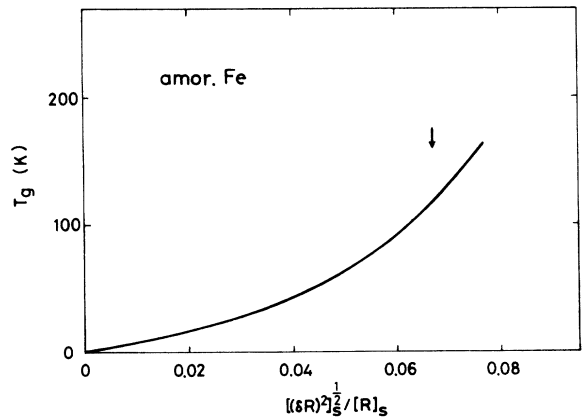

FIG. 12. The spin-glass temperature (T_g) as a function of the fluctuation $[(\delta R)^2]_s^{1/2}/[R]_s$. The arrow indicates the experimental (Ref. 41) and theoretical (Ref. 40) value. The curve was extrapolated below 25 K.

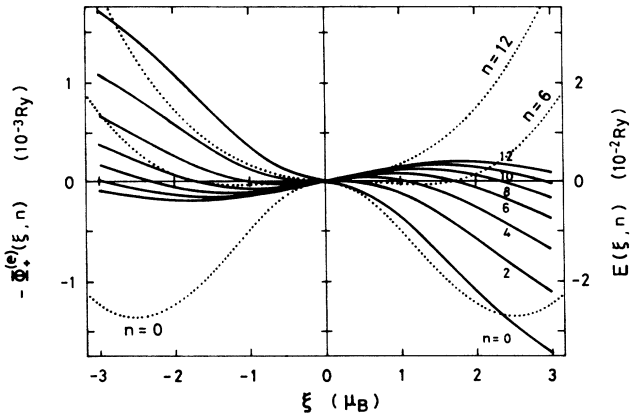

FIG. 13. Single-site energy [$E(\xi,n)$: dotted curves] and exchange pair energy [$-\Phi_+^{(e)}(\xi,n)$: solid curves] of amorphous iron in various environments (n) at $T=35$ K.

We examined the origin of the SG in amorphous iron by analyzing the energy functional $\Psi(\xi,nkl)$. The atomic pair energies $\Phi_\pm^{(a)}(\xi,n)$ in amorphous Fe are almost flat as a function of ξ. Thus, these terms are not essential for the spin configuration. We therefore show in Fig. 13 the energies $E(\xi,n)$ and $-\Phi_+^{(e)}(\xi,n)$. The former mainly determines the amplitude of LM in each local structure. The latter describes the exchange pair energy gain of the central LM ξ when the neighboring LM x points up. It is seen that $-\Phi_+^{(e)}(\xi,n)$ show a nonlinear behavior for the environments $4<n<10$; the LM's with large amplitude ($|\xi|$) ferromagnetically couple with the neighboring LM, while the LM's with small amplitude show the antiferromagnetic coupling. The same behavior has been found first in the fcc Fe alloys.[24,26] There the LEE on the amplitude of LM due to the atomic configuration caused the ferromagnetic and antiferromagnetic couplings via the nonlinear behavior of $\Phi_{\alpha\gamma}^{(e)}(\xi)$. In the present case the structural LEE causes the various amplitudes of LM's mainly via $E(\xi,n)$.

Let us draw a physical picture for Fe LM's from Fig. 13. The Fe atoms do not have their LM's in the environment $n=12$ since $E(\xi,12)$ shows a single minimum at $\xi=0$. In the environment $n=6$ the Fe atoms have a LM

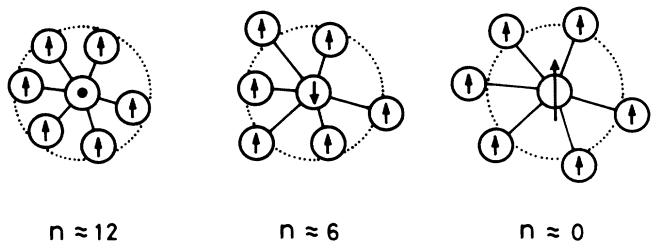

FIG. 14. Schematic representation showing the local environment effect on the central local moment (LM) in amorphous iron. n denotes the number of contracted atoms on the NN shell.

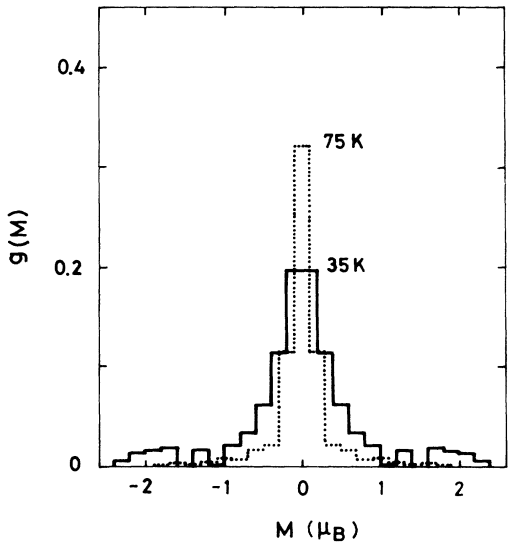

FIG. 15. The LM distribution in amorphous iron at $T=35$ and 75 K.

with small amplitude $\langle \xi^2 \rangle^{1/2} \approx 1.2\mu_B$ at low temperatures because $E(\xi,6)$ show the double minima at $\xi = \pm 1.2\mu_B$. These LM's show the antiferromagnetic coupling with neighboring LM since $-\Phi_+^{(e)}(\xi=-1.2,6) < -\Phi_+^{(e)}(\xi=1.2,6)$. On the other hand, the Fe atoms with the environment $n=0$ have well-defined LM with amplitude $\langle \xi^2 \rangle^{1/2} \approx 2.5$ as seen from $E(\xi,0)$ curves. These LM show the ferromagnetic couplings since $-\Phi_+^{(e)}(\xi=-2.5,0) > -\Phi_+^{(e)}(\xi=2.5,0)$. The obtained

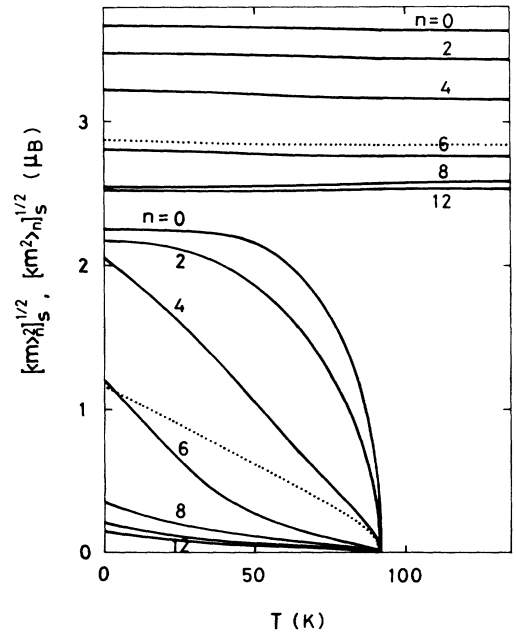

FIG. 16. The spin-glass order parameters ($[\langle m \rangle_n^2]_s^{1/2}$) and the amplitudes of the LM's ($[\langle m^2 \rangle_n]_s^{1/2}$) in various environments. Dotted curves denote the average values.

physical picture for couplings between Fe LM's is shown in Fig. 14. The coexistence of the ferromagnetic antiferromagnetic couplings due to the structural disorder give rise to the SG in amorphous iron. The mechanism mentioned above is characteristic to the metals since neither the LEE on the amplitude nor the nonlinearity of the magnetic coupling is seen in the insulators.

The detail of the LM distribution is shown in Fig. 15. The LM's show a broad distribution between $-2.5\mu_B$ and $2.5\mu_B$, and have a central peak which corresponds to the paramagnetic atoms. The latter peak grows up with increasing temperature, and becomes a δ-function peak above T_g.

The temperature variations of the root mean square of LM $\langle m \rangle$ for each environment n (i.e., $[\langle m \rangle_\pi^2]_s^{1/2}$) are shown in Fig. 16. The quantities $[\langle m \rangle_n^2]_s^{1/2}$ with contracted atoms $n > 6$ rapidly decrease with increasing temperature, while those for isolated atoms ($n < 2$) show Brillouin-like curves because of the strong ferromagnetic couplings to the neighboring Fe LM's. The amplitudes of LM's in various structural environments hardly change with increasing temperature, but their distributions spread from $2.5\mu_B$ to $3.7\mu_B$ as shown in Fig. 16. This broad distribution results from the fact that the amorphous iron is close to the Stoner criterion.

IV. SUMMARY AND DISCUSSION

We have generalized the finite-temperature theory of LEE to amorphous and liquid alloys, in which both the thermal spin fluctuations and the fluctuations of the LM's due to the structural disorder play an important role in their magnetic properties. The theory directly treats the structural disorder inside the NN shell by using the Bethe approximation to the electronic state and the method of distribution function for the LM distribution, while the structural disorder outside the cluster is treated by a self-consistent effective medium.

The present theory has a wide range of application. The theory covers the finite-temperature magnetism of crystals, substitutional alloy systems, amorphous systems, and liquid systems in both metallic and insulating states, since it takes into account the structural as well as configurational disorder on the basis of the functional-integral method. More important is that the theory describes the LM distribution and the SG state since it takes into account the LEE going beyond the single-site approximation. In particular, we have shown that the theory describes both types of the SG due to configurational and structural disorders, which reduce to the SG's in bond and site models in the insulator limit.

We have investigated the magnetic properties of amorphous iron by using the new theory. We have demonstrated that the local DOS, LM's, susceptibilities, and the amplitudes of LM's are strongly influenced by the LEE due to the structural disorder.

The amorphous iron does not show a stable ferromagnetism, but Fe LM's with various amplitudes are produced in amorphous iron because of the structural disorder. The Fe LM's with large amplitude show the ferromagnetic coupling and the Fe LM's with small am-

plitude show the antiferromagnetic couplings in amorphous iron. The coexistence of ferromagnetic and antiferromagnetic couplings between neighboring Fe LM's leads to the itinerant electron SG. The calculated transition temperature ($T_g \approx 100$ K) is consistent with those expected from the experimental data of Fe-rich amorphous alloys.

Quite recently, Krey, Krompiewski, and Krauss[34] have performed the ground-state Hartree-Fock calculations for amorphous Fe and Fe-Zr alloys, allowing for arbitrary LM configuration with transverse components. They obtained (1) the results for the z component approximately the same as the previous calculations without transverse components, (2) the existence of Fe LM's antiparallel to the magnetization, and (3) the metastable spin configurations suggesting the existence of the SG. These results support our results.[33]

However, they obtained finite magnetization (e.g., $[\langle m \rangle]_s = 1.4\mu_B$ for the density 8.0 g/cm^3) in disagreement with our results. A part of the finite magnetization is attributed to the very large magnetic field $h = 0.05$ eV/μ_B in their calculations, which is comparable to the Curie temperature of bcc Fe, but the discrepancy between the present results and their results seems to originate in the difference in the structural model and the method of calculation for the ground-state electronic structure between the theories.

Our calculations are based on Fujiwara's DOS for nonmagnetic amorphous iron.[7,52] He adopted the computer-generated structural model with 1500 atoms relaxed to metastable equilibrium, and calculated the ground-state electronic structure within the local-spin-density approximation to the density-functional theory by using the first-principles linear-muffin-tin-orbital method combined with the recursion method. The highest peak located at 0.043 Ry above the Fermi level has the value 46.5 (states/Ry atom). The DOS at the Fermi level is estimated to be $\rho(\varepsilon_F) = 28.2$ (states/Ry atom). Adopting the Stoner parameter $\tilde{J} = 0.068$ Ry (Ref. 55), we obtain the Stoner criterion $\tilde{J}\rho(\varepsilon_F)/2 = 0.96 < 1$.

On the other hand, Krey *et al.* adopted the computer-generated model of amorphous Fe which consists of 54 atoms in a box with periodic boundary conditions, and used the Slater-Koster tight-binding scheme with s, p, and d orbitals for the calculation of the electronic structure. The transfer integrals were parametrized to reproduce Wood's nonmagnetic bands[56] in the bcc Fe. The calculated DOS shows the highest peak just at the Fermi level, and has the value $\rho(\varepsilon_F) = 25.3$ (state/Ry atom). Using their Stoner parameter $\tilde{J} = 0.082$ Ry, we obtain the Stoner criterion $\tilde{J}\rho(\varepsilon_F)/2 = 1.04 > 1$ which might allow for the uniform polarization in contradiction to Fujiwara's result. The origin of the discrepancy has to be clarified in more details in the future.

The present theory established a method to calculate the magnetic properties of amorphous and liquid alloys at finite temperatures from the ground-state electronic structure. Application of our theory combined with the ground-state theories allows for the theoretical understanding of magnetism in amorphous and liquid alloys. In following works we plan to present the results of our systematic investigations for amorphous $3d$ transition metals and alloys.

ACKNOWLEDGMENTS

The author would like to thank Dr. V. L. Moruzzi and Professor T. Fujiwara for sending him their DOS for γ-Fe and amorphous Fe, respectively. He is also much indebted to Professor M. Matsuura, Professor K. Fukamichi, Dr. H. Wakabayashi, Professor T. Goto, Dr. N. Saito, and Professor Y. Nakagawa for informing him of their experimental data prior to publication.

[1] J. M. Ziman, *Models of Disorder* (Cambridge University Press, London, 1979).
[2] L. M. Roth, Phys. Rev. B **9**, 2476 (1974).
[3] S. Asano and F. Yonezawa, J. Phys. F **10**, 75 (1980).
[4] For a review of the recursion method see V. Heine, Solid State Phys. **35**, 1 (1980).
[5] For a review of the linear-muffin-tin-orbital method see H. L. Skriver, *The LMTO Method* (Springer, Berlin, 1984).
[6] T. Fujiwara, J. Phys. F **9**, 2011 (1979).
[7] T. Fujiwara, J. Non-Cryst. Solids **61&62**, 1039 (1984).
[8] R. H. Fairlie, W. M. Temmerman, and B. L. Gyorffy, J. Phys. F **12**, 1641 (1982).
[9] S. Krompiewski, U. Krey, and H. Ostermeier, J. Magn. Magn. Mater. **69**, 117 (1987); S. Krompiewski, U. Krey, U. Krauss, and H. Ostermeier, *ibid.* **73**, 5 (1988).
[10] For a review on the recent development of the metallic magnetism see *Metallic Magnetism*, edited by H. Capellmann (Springer, Berlin, 1987).
[11] Y. Kakehashi, Phys. Rev. B **40**, 11 063 (1989).
[12] M. Cyrot, J. Phys. (Paris) **33**, 25 (1972).
[13] J. Hubbard, Phys. Rev. **19**, 2626 (1979); **20**, 4584 (1979); **23**, 597 (1981).
[14] H. Hasegawa, J. Phys. Soc. Jpn. **46**, 1504 (1979); **49**, 178 (1980).
[15] J. M. D. Coey, F. Givord, A. Lienard, and J. P. Reboullat, J. Phys. F **11**, 2707 (1981).
[16] D. H. Ryan, J. M. D. Coey, E. Batalla, Z. Altounian, and J. O. Ström-Olsen, Phys. Rev. B **35**, 8630 (1987).
[17] N. Saito, H. Hiroyoshi, H. Fukamichi, and Y. Nakagawa, J. Phys. F **16**, 911 (1986).
[18] H. Wakabayashi, K. Fukamichi, H. Komatsu, T. Goto, T. Sakakibara, and K. Kuroda, *Proceedings of the International Symposium on the Physics of Magnetic Materials* (World-Scientific, Singapore, 1987), p. 342.
[19] Y. Kakehashi, J. Phys. Soc. Jpn. **50**, 3177 (1981).
[20] Y. Kakehashi, J. Magn. Magn. Mater. **37**, 189 (1983).
[21] Y. Kakehashi, J. Magn. Magn. Mater. **43**, 79 (1984).
[22] Y. Kakehashi, Phys. Rev. B **32**, 3035 (1985).
[23] Y. Kakehashi, Phys. Rev. B **35**, 4973 (1987).
[24] Y. Kakehashi, Phys. Rev. B **38**, 474 (1988).
[25] Y. Kakehashi and O. Hosohata, J. Phys. (Paris) Colloq. **49**, C8-73 (1988).
[26] Y. Kakehashi and O. Hosohata, Phys. Rev. B **40**, 9080 (1989).
[27] Y. Kakehashi, Phys. Rev. B **34**, 3243 (1986).

[28]F. Matsubara, Prog. Theor. Phys. **52**, 1124 (1974).
[29]S. Katsura, S. Fujiki, and S. Inawashiro, J. Phys. C **12**, 2839 (1979).
[30]K. Fukamichi, T. Goto, H. Komatsu, and H. Wakabayashi, *Proceedings of the Fourth International Conference on the Physics of Magnetic Materials,* edited by W. Gorkowski, H. K. Lachowicz, and H. Seymczak (World Scientific, Singapore, 1989), p. 354.
[31]S. Ishio, K. Nushiro, and M. Takahashi, J. Phys. F **16**, 1093 (1986).
[32]M. Acet, W. Stamm, H. Zahres, and E. F. Wassermann, J. Magn. Magn. Mater. **68**, 233 (1987).
[33]Y. Kakehashi, Phys. Rev. B **40**, 11 059 (1989).
[34]U. Krey, S. Krompiewski, and U. Krauss (unpublished).
[35]M. C. Gutzwiller, Phys. Rev. Lett. **10**, 159 (1963).
[36]J. Hubbard, Proc. R. Soc. London, Ser. A **276**, 238 (1963).
[37]R. L. Stratonovich, Dokl. Akad. Nauk SSSR **115**, 1097 (1958) [Sov. Phys.—Dokl. **2**, 416 (1958)].
[38]J. Hubbard, Phys. Rev. Lett. **3**, 77 (1959).
[39]H. Shiba, Prog. Theor. Phys. **46**, 77 (1971).
[40]R. Yamamoto and M. Doyama, J. Phys. F **9**, 617 (1979).
[41]M. Matsuura, H. Wakabayashi, T. Goto, H. Komatsu, and K. Fukamichi, J. Phys. Cond. Mat. **1**, 2077 (1989).
[42]H. Miwa, J. Magn. Magn. Mater. **10**, 223 (1979).
[43]N. Hamada and H. Miwa, Prog. Theor. Phys. **59**, 1045 (1978).
[44]N. Hamada, J. Phys. Soc. Jpn. **46**, 1759 (1979).
[45]Y. Kakehashi, J. Phys. Soc. Jpn. **50**, 1505 (1981).
[46]A. Bieber and F. Gautier, Solid State Commun. **39**, 149 (1981).
[47]P. Soven, Phys. Rev. **156**, 809 (1967); B. Velicky, S. Kirkpatrick, and H. Ehrenreich, *ibid.* **175**, 747 (1968).
[48]H. Miwa, Prog. Theor. Phys. **52**, 1 (1974).
[49]J. M. Cowley, Phys. Rev. **77**, 669 (1950).
[50]S. F. Edwards and P. W. Anderson, J. Phys. F **5**, 965 (1975).
[51]D. Sherrington and S. Kirkpatrick, Phys. Rev. Lett. **35**, 1972 (1975).
[52]T. Fujiwara (unpublished).
[53]V. L. Moruzzi, Phys. Rev. Lett. **57**, 2211 (1986); V. L. Moruzzi, P. M. Marcus, K. Schwarz, and P. Mohn, Phys. Rev. B **34**, 1784 (1987); (private communication).
[54]U. K. Poulsen, J. Kollár, and O. K. Andersen, J. Phys. F **6**, L241 (1976).
[55]J. F. Janak, Phys. Rev. B **16**, 255 (1977).
[56]J. H. Wood, Phys. Rev. **126**, 517 (1962).